

Design principles of biochemical oscillators

Béla Novák* and John J. Tyson†

Abstract | Cellular rhythms are generated by complex interactions among genes, proteins and metabolites. They are used to control every aspect of cell physiology, from signalling, motility and development to growth, division and death. We consider specific examples of oscillatory processes and discuss four general requirements for biochemical oscillations: negative feedback, time delay, sufficient 'nonlinearity' of the reaction kinetics and proper balancing of the timescales of opposing chemical reactions. Positive feedback is one mechanism to delay the negative-feedback signal. Biological oscillators can be classified according to the topology of the positive- and negative-feedback loops in the underlying regulatory mechanism.

Somites

Early segmentations of the body of a vertebrate embryo that are laid down in a temporally and spatially periodic pattern.

Robustness

The notion that a control system should function reliably in the face of expected perturbations from outside the control system and from inevitable internal fluctuations.

Biochemical oscillations occur in many contexts (such as metabolism, signalling and development) and control important aspects of cell physiology, such as circadian rhythms, DNA synthesis, mitosis and the development of somites in vertebrate embryos (TABLE 1). In the 1950s and 1960s, the first clear examples of biochemical oscillations (in metabolic systems) were recognized in glycolysis^{1,2}, cyclic AMP production³ and the horseradish peroxidase reaction^{4,5}. Soon after these discoveries were made, theoreticians were thinking about the general requirements for chemical oscillations and the specific mechanisms of these examples^{6,7}. After the molecular biology revolution of the 1980s, many new examples of oscillations in protein-interaction networks (PINs) and in gene-regulatory networks (GRNs) came to light, such as the period (PER) proteins in animal circadian control⁸, the cyclin proteins in eukaryotic cell-cycle control^{9,10} and the repressilator¹¹ in genetically engineered bacteria.

Understanding the molecular basis of cellular oscillations is more than an exercise in experimental genetics and biochemistry. Oscillators have systems-level characteristics (for example, periodicity, robustness and entrainment) that transcend the properties of individual molecules or reaction partners and that involve the full topology of the reaction network. These properties can only be fully understood by viewing experimental data from a theoretical perspective and by quantitative mathematical modelling of chemical oscillatory processes. These models address general concepts of dynamical systems, such as feedback, time delays, bistability and hysteresis.

In this review, we present a series of examples of increasing complexity that illustrate the essential

requirements for biochemical oscillators. First, negative feedback is necessary to carry a reaction network back to the 'starting point' of its oscillation. Second, the negative-feedback signal must be sufficiently delayed in time so that the chemical reactions do not settle on a stable steady state. Third, the kinetic rate laws of the reaction mechanism must be sufficiently 'nonlinear' to destabilize the steady state. Fourth, the reactions that produce and consume the interacting chemical species must occur on appropriate timescales that permit the network to generate oscillations. Time delay can be created by a physical constraint (for example, the minimal time necessary to carry out transcription and translation, or the time needed to transport chemical species between cellular compartments), by a long chain of reaction intermediates (as in a metabolic pathway) or by dynamical hysteresis (overshoot and undershoot, as consequences of positive feedback in the reaction mechanism).

To keep the mathematical details of oscillating chemical reactions to a minimum, we will demonstrate the design principles of biochemical oscillators by rate plots (which show how reaction rates depend on chemical concentrations), signal-response curves (which show how oscillations turn on and off in response to regulatory signals) and 'constraint' diagrams (which show how the kinetic constants of a reaction mechanism are constrained by requirements for periodicity). The mathematics are available to interested readers in [Supplementary information S1–S4](#) (boxes). For further details on the principles that underlie chemical and biochemical oscillations, we refer readers to books^{12–15} and review articles^{2,6,16–18}.

*Oxford Centre for Integrative Systems Biology, Department of Biochemistry, University of Oxford, South Parks Road, Oxford OX1 3QU, UK.

†Department of Biological Sciences, Virginia Polytechnic Institute & State University, Blacksburg, Virginia 24061, USA.

Correspondence to B.N.

e-mail:

bela.novak@bioch.ox.ac.uk
doi:10.1038/nrm2530

Published online
30 October 2008

Table 1 | Survey of biochemical oscillators

Function	Components	Period	Class*	References
Metabolism	Glucose, ATP, phospho-fructokinase	2 min	3	52–54
Signalling	Cyclic AMP, receptor, adenylate cyclase	5 min	3	55,64
Signalling	Ca ²⁺ , Ins(1,4,5)P ₃	> 1 s	3	65
Signalling	NF-κB, IκB, IKK	~2 h	1	41,43
Signalling	p53, MDM2	5 h	1	39,40
			3	58,59
Signalling	Msn2, adenylate cyclase, cAMP, PKA	~10 min	1	66,67
Somitogenesis	Her1, Her7, Notch	30–90 min	1	40,68
Yeast endoreplication cycles	Cig2, Cdc10, Rum1	1–2 h	2	49
Frog egg cycles	CycB, Wee1, Cdc25, Cdc20	30 min	2	47, 48
Circadian rhythm	PER, TIM, CLOCK, CYC	24 h	1	26
			2	30

*See FIG. 5. Class 1 represents delayed negative-feedback loops; class 2 represents amplified negative-feedback loops; class 3 represents incoherently amplified negative-feedback loops. IκB, inhibitor of NF-κB; IKK, IκB kinase; Ins(1,4,5)P₃, inositol-1,4,5-triphosphate; NF-κB, nuclear factor κB.

Negative feedback with time delay

To lay bare the ‘design principles’ of biochemical oscillators, it does not make sense to start with a fully detailed model of a particular cellular rhythm, such as the cell cycle in human fibroblasts, which is likely to be so overlaid by subtle control signals that the essential features of the oscillator will be obscure. Rather, we start from a highly idealized model of periodic protein synthesis that illustrates the basic requirements of biochemical oscillators in their pristine forms.

We consider a protein (for example, *PER* in the circadian control system of fruit flies^{19,20}) that represses the transcription of its own gene (FIG. 1a). The details of this feedback repression are not important at present. The time-rate of change of protein concentration, dY/dt , is given by a simple kinetic equation:

$$\frac{dY}{dt} = k_1 S \frac{K_d^p}{K_d^p + Y^p} - k_2 E_T \frac{Y}{K_m + Y} \quad (1)$$

In this equation, the first term is the rate of protein synthesis and the second is its rate of degradation. The synthesis rate is proportional to a signal (S ; which might be the concentration of a transcription factor that upregulates the gene) multiplied by a factor, $K_d^p / (K_d^p + Y^p)$, which expresses how gene transcription is downregulated by protein Y . In this factor, K_d is the dissociation constant for the binding of Y to the upstream regulatory sequence of the gene, and p is an integer indicating whether Y binds to the DNA sequence as a monomer, dimer, trimer, or so on. The rate constant k_1 is the rate of synthesis of Y (per unit signal strength) when the concentration of Y is small and the gene is fully expressed. In the second term, E is a protease that degrades Y (E_T is the total concentration of enzyme), its turnover rate is k_2 and its Michaelis constant is K_m .

In FIG. 1b we plot the rates of synthesis and degradation of the protein Y as functions of the protein concentration, Y . From the diagram it is clear that the protein concentration, if indeed it is governed by equation 1,

will be drawn towards its steady-state value, Y_0 , without any oscillations, nor with any overshoots or undershoots. This is great if we are modelling ‘homeostasis’, but not if we want to model ‘oscillations’.

Explicit time delay. Suppose that the rate of protein synthesis at present (at time t) depends on the concentration of protein at some time in the past (at time $t - \tau$), where τ is the time delay that is required for transcription and translation. Then, the governing kinetic equation becomes:

$$\frac{dY(t)}{dt} = k_1 S \frac{K_d^p}{K_d^p + Y(t-\tau)^p} - k_2 E_T \frac{Y(t)}{K_m + Y(t)} \quad (2)$$

This model of protein synthesis and degradation was first studied in detail by Mackey and Glass in 1977 (REF. 21). For a proper choice of rate constants and time delay, this equation exhibits periodic oscillations, as illustrated in FIG. 1c. The time delay causes the negative-feedback control repeatedly to overshoot and undershoot the steady state (FIG. 1d). For details on how to simulate equation 2 and all other models in this review, see [Supplementary information S1](#) (box).

By ‘proper choice of rate constants’ we mean that for $Y(t)$ to oscillate, the kinetic parameters — S (signal strength), p (nonlinearity of feedback), K_m (nonlinearity of the removal step) and τ (duration of time delay) — must satisfy specific constraints, as illustrated in FIG. 1e,f. For details on how these constraint curves are calculated, see [Supplementary information S2](#) (box). The constraints can be summarized in three requirements. First, the time delay, τ , must be sufficiently long. (For fixed values of p and K_m , there is a minimum value of τ , τ_{\min} , below which oscillations are impossible.) Second, the reaction rate laws must be sufficiently ‘nonlinear’. (Oscillations become easier — that is, τ_{\min} gets smaller — as either p or K_d/K_m increases.) Third, the rates of opposing processes must be appropriately balanced.

Entrainment

The process whereby two interacting oscillating systems, which have different periods when running independently, assume the same period. The two oscillators may fall into synchrony, but other phase relationships are also possible.

Bistability

A reaction network with two coexisting stable steady states (separated by an unstable steady state). Which stable state the network adopts depends on the initial concentrations of the reacting species.

Hysteresis

A property of systems with bistability. The control system can be switched from one stable state to the other by a transient signal, and switched back again by a different transient signal. Hence, the state of the system depends not only on its present conditions, but also on its recent history.

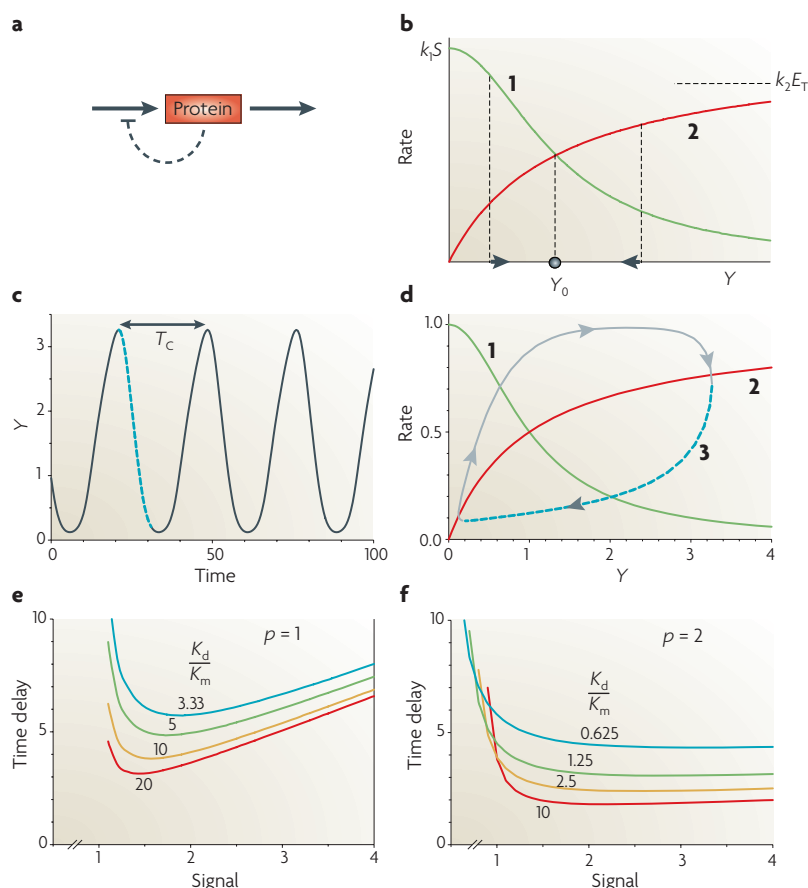


Figure 1 | Time-delayed negative-feedback oscillator. **a** | The protein level is determined by opposing processes of synthesis and degradation. Protein synthesis is downregulated by the protein itself. **b** | Curves 1 and 2 represent the rates of protein synthesis and degradation, respectively. The arrows indicate the direction of change of protein concentration, which is always towards Y_0 , the steady state concentration of protein, where the rate of synthesis equals the rate of degradation. **c** | Sustained oscillations for equation 2, with $p = 2$, $K_d/K_m = 1$, $S/K_d = 1$, $k_1 = k_2 E_T/K_d = 1 \text{ min}^{-1}$ and $\tau = 10 \text{ min}$. The period of oscillation, T_c , is 27.2 min. **d** | In curve 3 we plot the time-delayed rate of protein synthesis, $1/(1+Y(t-\tau)^p)$, as a function of the present protein concentration, $Y(t)$. The dashed portion of curve 3 corresponds to the dashed portion of the oscillation in panel c; it is τ time units in duration, and it extends from the maximum value of Y (at $t = 20 \text{ min}$) to the minimum value of the rate of production of Y (at $t = 30 \text{ min}$). The time-delayed loop repeatedly overshoots and undershoots the steady state because the protein synthesis rate is no longer given by curve 1 at $Y(t)$, but instead is given by curve 1 at $Y(t-\tau)$. **e** | Constraint curves for $p = 1$. Each curve is drawn for a specific value of K_d/K_m . For each case, equation 2 exhibits sustained oscillations in the region above the curve. **f** | Constraint curves for $p = 2$. Notice that the oscillatory domain becomes larger as p increases and as K_d/K_m increases; that is, as the kinetic rate laws become more nonlinear. E_T , the total concentration of enzyme; k_1 , the rate of synthesis of protein Y ; k_2 , the enzyme's turnover rate; K_d , the dissociation constant; K_m , the Michaelis constant; p , an integer indicating whether Y binds to the DNA sequence as a monomer, dimer, trimer, or so on; S , the signal strength; t , the time variable; τ , the duration of time delay.

To understand the third requirement, we must look more closely at the axes in FIG. 1e,f. The value of the 'time delay' plotted on the vertical axis is really a dimensionless combination of parameters:

$$\frac{k_2 E_T \tau}{K_d} = \frac{\tau}{K_d/k_2 E_T} = \frac{\tau}{T_{\text{degr}}} = \frac{\text{time delay}}{\text{time scale for protein degradation}} \quad (3)$$

The value of 'signal strength' plotted on the horizontal axis is the dimensionless ratio:

$$\frac{k_1 S}{k_2 E_T} = \frac{K_d/k_2 E_T}{K_d/k_1 S} = \frac{T_{\text{degr}}}{T_{\text{syn}}} = \frac{\text{time scale for protein degradation}}{\text{time scale for protein synthesis}} \quad (4)$$

For fixed values of p and K_d/K_m , these ratios must lie above a specific curve plotted in FIG. 1e,f. For example, for $p = 2$ and $K_d/K_m = 10$ ('modest' nonlinearity of the rate laws for protein synthesis and degradation), these ratios must (roughly speaking) satisfy the inequalities: $\tau/T_{\text{degr}} > 2$ and $T_{\text{degr}}/T_{\text{syn}} > 1$ (from the lowest curve in FIG. 1f). Estimating the time delay for transcription and translation to be $\sim 20 \text{ min}$, we predict that for the negative-feedback loop to oscillate, the timescale for protein degradation must be $< 10 \text{ min}$ and the timescale for protein synthesis must be even shorter. If these conditions are satisfied, then the period of oscillation is (again, roughly speaking) between twice and four times the time delay; that is, $\sim 40\text{--}80 \text{ min}$.

In the remainder of this review, we intend to show that these four elements (negative feedback, nonlinearity, time delay and timescale constraints) are generally needed for all biochemical oscillators, provided the notion of time delay is suitably generalized.

Time delay by a series of intermediates. Our simple model of negative feedback on gene expression in equation 2 exhibits sustained oscillations if there is a sufficiently long time delay between the action of the protein Y on the gene and the appearance of new protein molecules in the cytoplasm. We express this requirement as a discrete time delay, τ , in the kinetic equation. Maybe we can dispense with τ if we include the dynamics of mRNA in our model (FIG. 2a). To this end, we write a pair of kinetic equations for X = mRNA concentration and Y = protein concentration:

$$\frac{dX}{dt} = k_1 S \frac{K_d^p}{K_d^p + Y^p} - k_{\text{dx}} X \quad (5)$$

$$\frac{dY}{dt} = k_{\text{sy}} X - k_2 E_T \frac{Y}{K_m + Y}$$

In these equations, k_{dx} and k_{sy} are the rate constants for degradation of mRNA and synthesis of proteins, respectively.

In FIG. 2b we plot the 'nullclines' of this pair of nonlinear differential equations. The X -nullcline (curve 1 in FIG. 2b) is the locus of points in the (XY) plane where the rate of mRNA synthesis is exactly balanced by the rate of mRNA degradation; that is, where:

$$X = \frac{k_1 S}{k_{\text{dx}}} \frac{K_d^p}{K_d^p + Y^p} \quad (6)$$

Along the X -nullcline, $dX/dt = 0$ and trajectories move horizontally in the (XY) plane because there is no change in the X direction but there may be change in the Y direction. The Y -nullcline (curve 2 in FIG. 2b) is the locus of points where the rate of protein synthesis is balanced by the rate of degradation; that is, where:

$$X = \frac{k_2 E_T}{k_{\text{sy}}} \frac{Y}{K_m + Y} \quad (7)$$

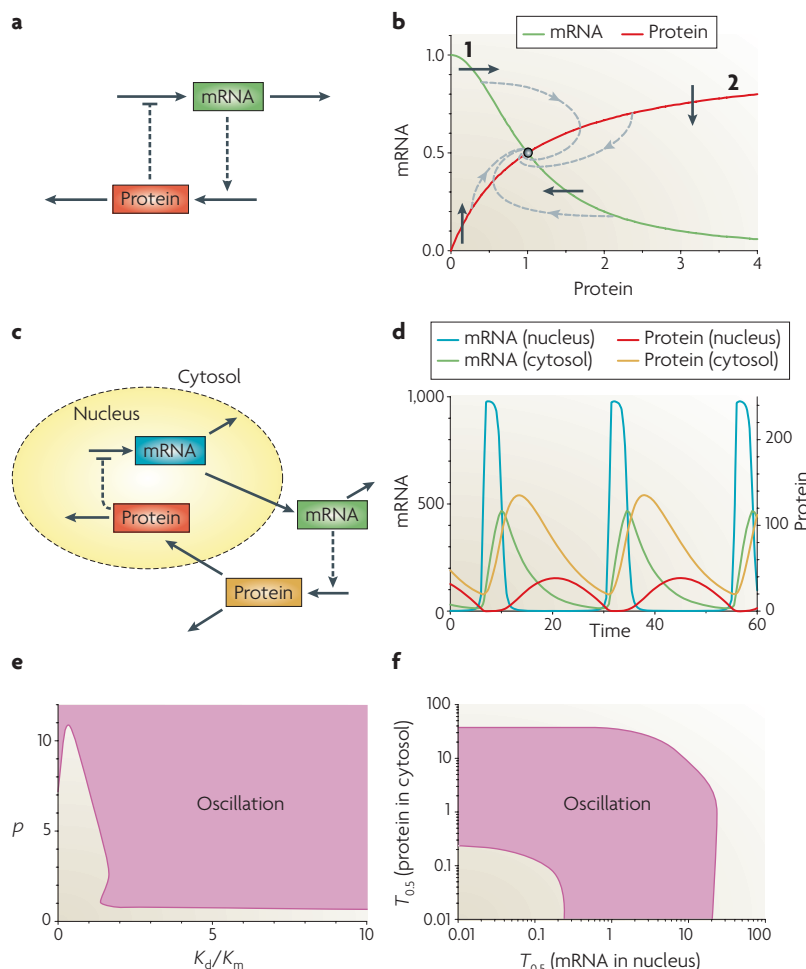


Figure 2 | Multi-component negative-feedback oscillator. **a** | Negative feedback between mRNA and protein, as described by kinetic equations 5. **b** | Representative solutions (dashed curves) of equations 5, for parameter values: $p = 2$, $K_m/K_d = 1$, $S/K_d = 1$, $k_1 = k_{dx} = 0.1 \text{ min}^{-1}$, $k_{sy} = k_2 E_T/K_d = 1 \text{ min}^{-1}$. Notice that every trajectory spirals into the stable steady state located at the grey circle. Curves 1 and 2 are ‘nullclines’ for differential equations 5, as explained in the main text. The small arrows indicate the direction of motion of trajectories as they cross the nullclines. Notice that the nullclines in this figure are identical to the rate curves in FIG. 1b. **c** | The negative-feedback loop, taking into account transport of macromolecules between the nucleus and the cytoplasm. **d** | Sustained oscillations for the four-component loop in panel **c**. See [Supplementary information S1](#) (box) for details. **e** | Nonlinearity constraint. For the negative-feedback loop to oscillate, p and K_d/K_m must be sufficiently large. **f** | Timescale balancing constraint. The half-lives ($T_{0.5}$) of mRNA in the nucleus and of protein in the cytoplasm must lie in the shaded band for the negative-feedback loop to oscillate. E_T , the total concentration of enzyme; k_1 , the rate of synthesis of protein Y ; k_2 , the enzyme’s turnover rate; K_d , the dissociation constant; k_{dx} , the turnover rate of mRNA; K_m , the Michaelis constant; k_{sy} , the rate for the synthesis of protein; p , an integer indicating whether Y binds to the DNA sequence as a monomer, dimer, trimer, or so on; S , the signal strength.

Along the Y -nullcline, $dY/dt = 0$ and trajectories move vertically in the (XY) plane. Where the nullclines intersect (the solid circle in FIG. 2b), the trajectory comes to rest at a steady state ($dX/dt = 0$ and $dY/dt = 0$). The sample trajectories in FIG. 2b (the dashed lines) spiral into the steady state. Although the system of reactions may exhibit dampened oscillations on the way to the steady state, sustained oscillations in this simple gene regulatory circuit are impossible²². Hence, adding mRNA

to the model does not do away with the requirement for an explicit time delay.

Before giving up the idea of replacing the time delay by a series of intermediates in the negative-feedback loop, let us recognize that (in eukaryotes) the mRNA and protein molecules need to be transported between the nucleus and cytoplasm (FIG. 2c). Equations 5 are readily expanded to four variables: mRNA and protein in the nucleus (X_n , Y_n) and in the cytoplasm (X_c , Y_c). The four-variable negative-feedback loop oscillates as naturally as a pendulum (FIG. 2d).

The constraint diagrams in FIG. 2 underscore the conclusions of the previous section. FIG. 2e shows that the kinetic rate laws must be sufficiently nonlinear (that is, p and/or K_d/K_m are sufficiently large). FIG. 2f shows that the half-lives of mRNA in the nucleus and protein in the cytoplasm must be properly balanced. If either half-life becomes very short (that is, if either component turns over very rapidly), then that component maintains its steady-state value and the feedback loop reduces to three components, either ‘ X_c , Y_c , Y_n ’ or ‘ X_n , X_c , Y_n ’. Nonetheless, oscillations persist. Hence, we conclude that oscillations are impossible in a two-component negative-feedback loop (FIG. 2b), but are possible in a three-component negative-feedback loop²² (FIG. 2f).

This mechanism (negative feedback on gene expression with three or more components in the feedback loop), which we have used to illustrate the four basic principles of biochemical oscillations, was first put forward by Brian Goodwin^{23,24} in the mid-1960s as a model for periodic enzyme synthesis in bacteria. Our calculations in this section show that, with an effective time delay (due to transcription, translation and transport of reaction intermediates) of ~ 20 min, this model gives a period of ~ 1 h, which is close to the observed periods of such rhythms²⁵. This mechanism has also been a favourite model for circadian rhythms in flies and mammals, governed by the PER protein, which moves into the nucleus and blocks expression of the *PER* gene^{26,27}. Of course, to get a period of 24 h, the time delay for the feedback signal must be considerably longer than the delay expected for transcription, translation and nuclear transport. It is thought that PER undergoes slow post-translational modifications (phosphorylations) in the cytoplasm before it returns to the nucleus²⁰.

The possibility of sustained oscillations in a three-component negative-feedback loop was used by Elowitz and Leibler¹¹ to design the ‘repressilator’, a synthetic GRN in *Escherichia coli* that consists of three operons, each one expressing a protein that represses the next operon in the loop. The successful engineering of the repressilator was a foundational triumph of the nascent field of synthetic biology and a vindication of the theoretical ideas of Goodwin^{23,24}, Griffith²², Goldbeter²⁶ and others.

Time delay by positive feedback. Time delay is a sort of memory: protein synthesis rate at the present time depends on protein concentration over some time in the past. Memory is a property of biochemical systems with bistability: under identical chemical conditions, the system can be in either of two alternative stable states^{28,29}.

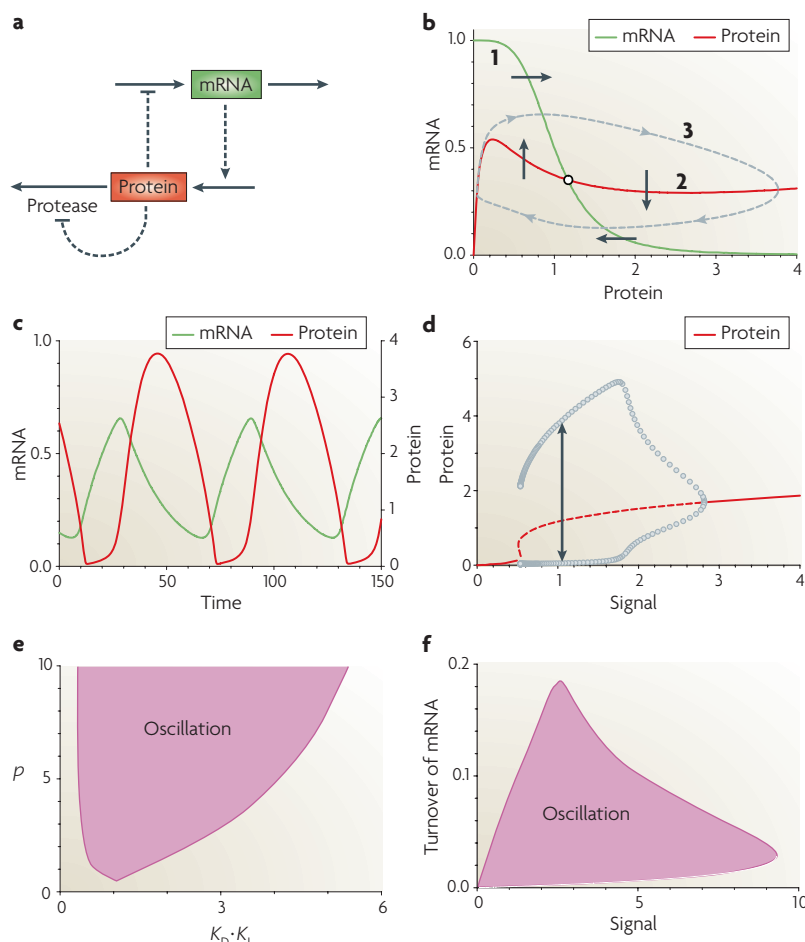


Figure 3 | Hysteresis-driven negative-feedback oscillator. **a** | RNA and protein in a negative-feedback loop, as in FIG. 2. This mechanism is described by kinetic equations 8. **b** | Limit cycle solution (curve 3) of equations 8 for parameter values: $p = 4$, $K_m/K_d = 0.1$, $K_d \cdot K_i = 2$, $S = 1$, $k_1 = k_d = k_{dy} = 0.05 \text{ min}^{-1}$, $k_{sy} = k_2 E_T / K_d = 1 \text{ min}^{-1}$. Curves 1 and 2 as in FIG. 2b, except that curve 2 is given by $X = k_{dy} + Y / (K_m + Y + K_i Y^2)$. **c** | Sustained oscillations of mRNA and protein, corresponding to curve 3 in panel **b**. **d** | Signal-response curve. Solid lines represent stable steady states; dashed lines represent unstable steady states; grey circles represent maximum and minimum excursions of $Y(t)$ during a limit cycle oscillation. The oscillation in panel **c** is indicated by the double-headed arrow at $S = 1$. Notice that oscillations are possible only for a restricted range of S . **e** | Nonlinearity constraint. For this mechanism to oscillate, the positive-feedback loop must be strong enough (K_i must be sufficiently large) and the negative-feedback loop must be sufficiently nonlinear (p must be sufficiently large). **f** | Timescale balancing constraint. The turnover rate of mRNA (k_{dx}) cannot be too large, and S must be within specific bounds for this system to oscillate. E_T , the total concentration of enzyme; k_1 , the rate of synthesis of protein Y ; k_2 , the enzyme's turnover rate; K_d , the dissociation constant; k_{dx} , the turnover rate of mRNA; k_{dy} , the rate constant for an alternative pathway of protein degradation; K_i , a constant characterizing the strength of inhibition of enzyme E by its substrate; K_m , the Michaelis constant; k_{sy} , the rate for the synthesis of protein; p , an integer indicating whether Y binds to the DNA sequence as a monomer, dimer, trimer, or so on; S , the signal strength; t , the time variable; X and Y , the concentrations of mRNA and protein, respectively.

Which state a system occupies depends on its recent history (a phenomenon called hysteresis). Hysteresis can prevent a system with negative feedback from finding its homeostatic steady state. To see how this happens, we add positive feedback to our mRNA-protein system in equation 5. In particular, we assume that protein Y , in addition to binding to its own gene regulatory site and downregulating its own expression, can bind to

an allosteric site on protease E and thereby inhibit the activity of E (FIG. 3a). The kinetic equations become:

$$\begin{aligned} \frac{dX}{dt} &= k_1 S \frac{K_d^p}{K_d^p + Y^p} - k_{dx} X \\ \frac{dY}{dt} &= k_{sy} X - k_{dy} Y - k_2 E_T \frac{Y}{K_m + Y + K_i Y^2} \end{aligned} \quad (8)$$

In these equations, k_{dy} is the rate constant for an alternative pathway of protein degradation and K_i is a constant that characterizes the strength of the inhibition of enzyme E by its substrate Y . In equation 8, as before, S is the concentration of a transcription factor that upregulates the expression of the mRNA that encodes protein Y . We think of S as a signal that can induce sustained oscillations in protein level as a function of time.

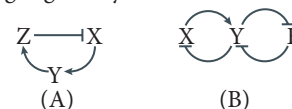
In FIG. 3b we draw the nullclines of equations 8 in the same format as FIG. 2b. The effect of positive feedback is a kink in the degradation curve (compare curves 2 in FIGS 2b, 3b), and the kink forces the dynamical system to overshoot and undershoot the steady state repeatedly (compare the dashed trajectories in FIGS 2b, 3b). The system executes sustained oscillations (FIG. 3c), provided the signal strength, S , is within certain bounds (FIG. 3d).

The constraint diagrams (FIG. 3e,f) show that these oscillations require positive feedback (they disappear if K_i is too small or too large) and proper balancing of timescales (mRNA must be sufficiently stable (k_{dx} must not be too large), and signal strength must lie within strict bounds (S must not be too large or too small)).

This mechanism (negative feedback on gene expression plus inhibition of protein degradation) has been suggested by Tyson *et al.*³⁰ as a possible source of circadian rhythms in the reaction network that governs expression of the *PER* gene in fruit flies. Their idea was that the *PER* protein may form dimers that are less prone to degradation by the protease (E in the model is casein kinase, which phosphorylates *PER* and labels it for proteolysis). Other examples of this design for oscillations will be given after we expand our notion of reaction mechanisms from gene regulation to metabolic control systems (MCSs) and PINs.

Biochemical interaction networks

Using a simple GRN as an example, we have discovered two distinct mechanisms for generating oscillations: a negative-feedback loop with at least three components, and a combination of short positive- and negative-feedback loops. We might depict these mechanisms with the following 'regulatory motifs':



In these motifs, $X \rightarrow Y$ means 'X activates Y' and $X \rightarrow Y$ means 'X inhibits Y'. The general ideas discussed in the previous section — positive and negative feedback, time delay and nonlinearity — are not limited to GRNs but apply equally well to MCSs and to PINs. We would like to know whether there is a general theory of regulatory motifs (like the two above) that classifies types of biochemical oscillator.

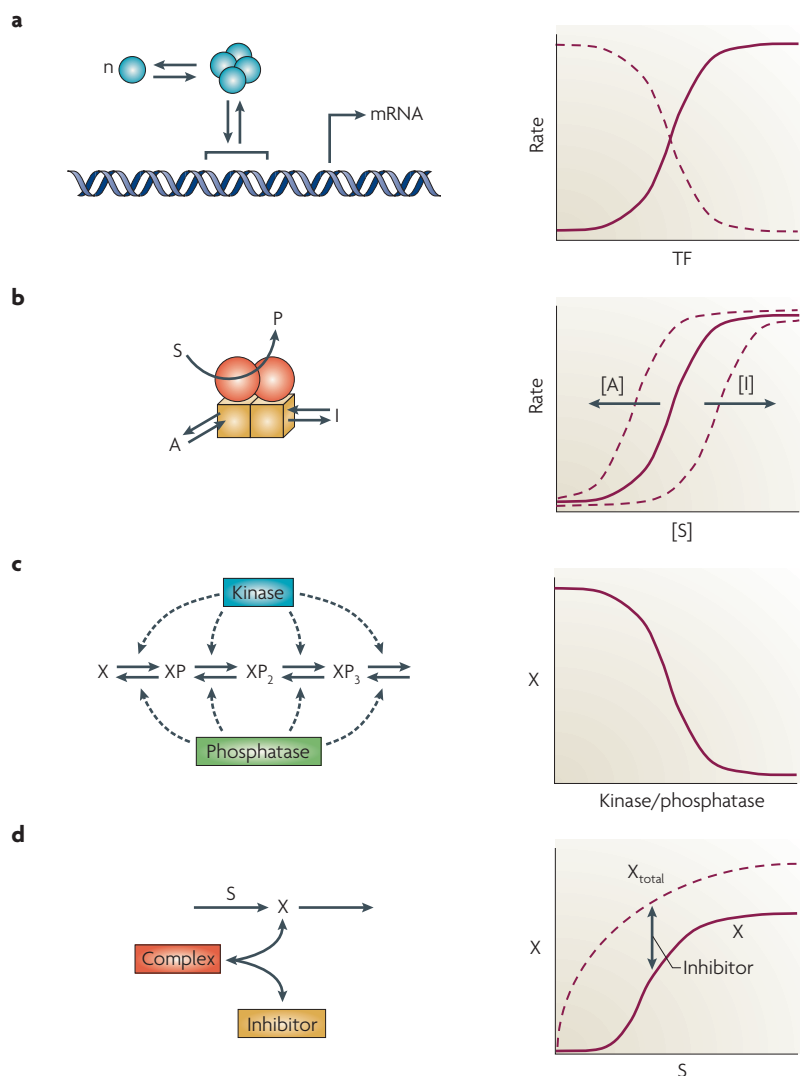


Figure 4 | Sources of nonlinearity. **a** | Oligomer binding. Left: a transcription factor (blue ball) forms an n -component homo-oligomer, which then binds upstream of a structural gene and either activates or represses mRNA synthesis. Right: the rate of mRNA synthesis as a function of transcription factor (TF) concentration, for an activator (solid line) or a repressor (dashed line). **b** | Cooperativity and allostery. Left: an enzyme, consisting of two catalytic subunits (spheres) and two regulatory subunits (cubes), catalyses the conversion of substrate (S) into product (P). Activators (A) and inhibitors (I) bind to specific sites on the regulatory subunits. Right: if the binding of substrate to the catalytic subunits is cooperative, then the rate of reaction as a function of substrate concentration is sigmoidal (solid line). The rate curve can be shifted to the left or to the right by increasing the concentration of the activator or inhibitor, respectively. **c** | Multisite phosphorylation. Left: a regulatory protein, X, is phosphorylated on multiple sites by a protein kinase and is dephosphorylated by a protein phosphatase. Right: the concentration of the unphosphorylated form of X as a function of the ratio of activities of kinase and phosphatase. **d** | Stoichiometric inhibition. Left: a regulatory protein, X, is synthesized in response to a signal, S. X binds strongly to an inhibitor to form an inactive complex. Right: the concentration of total X increases hyperbolically with S (dashed line), but the concentration of 'free' X is a sigmoidal function of S (solid line).

In this review we are not so much interested in the precise mechanisms of particular biochemical oscillators as we are in the patterns of activation and inactivation (that is, the regulatory motifs) that appear repeatedly in all known oscillators. How activation and inhibition are achieved biochemically varies considerably, depending on

the context. In GRNs, transcription factors bind to regulatory sequences upstream of genes and control whether the gene is transcribed to mRNA or not. In MCSs, metabolites bind to enzymes and control how quickly or slowly the enzyme catalyses a particular chemical reaction. In this way, metabolite X can 'activate' metabolite Y either by activating the enzyme that produces Y or by inhibiting the enzyme that consumes Y. In PINs, protein X might activate protein Y because X is a kinase that phosphorylates Y, or because X is a binding partner that forms an active X–Y dimer. Protein X might, just as well, inactivate protein Y by binding to Y, by phosphorylating Y or by degrading Y. Given all these possibilities, there are many ways to build a PIN or MCS to instantiate a particular regulatory motif. The examples discussed above, which involve negative feedback on gene expression, suggest that besides the regulatory motif itself (the pattern of positive and negative interactions), an oscillatory mechanism must have sufficient 'nonlinearity' and the rates of particular opposing reactions must be properly balanced.

Nonlinearities arise in biochemical reaction networks from many sources (FIG. 4). We have already used the example of a multimeric transcription factor binding to a genetic regulatory sequence (FIG. 4a), for which the probability of binding is given by a nonlinear so-called Hill function³¹, $S^n / (K_d^n + S^n)$. Cooperative binding of substrates and modifiers to multisubunit allosteric enzymes (FIG. 4b) also generates sigmoidal nonlinearities, adequately described by Hill functions or by more accurate kinetic rate laws^{31,32}. Reversible phosphorylation and dephosphorylation of target molecules can create a sigmoidal signal–response curve if the interconverting enzymes (kinases and phosphatases) have high affinity (low K_m) for their abundant substrates (zero-order ultrasensitivity³³) or if the target molecule has multiple phosphorylation sites³⁴ (FIG. 4c). Our final example is a stoichiometric inhibitor that binds to a regulatory protein (X) to form an inactive complex (FIG. 4d): as the total amount of X increases in response to a signal, the active fraction of X shows a highly nonlinear signal–response curve³⁵. A high-affinity substrate can work as a stoichiometric inhibitor of its enzyme, making enzyme activity for other substrates nonlinearly dependent on the enzyme level³⁶. These sorts of interactions, when introduced into reaction networks of the right topology, may provide the nonlinearity that is needed to generate oscillations.

Next we present a general classification scheme for simple regulatory motifs that exhibit sustained oscillations, provided the chemical implementation has sufficient nonlinearity (introduced by reactions such as those in FIG. 4) and that the timescales of the reactions are properly balanced.

Classification of oscillatory motifs

So far we have used examples to show that biochemical oscillations can be generated by a delayed negative-feedback loop (with at least three components in the loop) or by combining positive- and negative-feedback loops. In this section, we want to put these two examples into a general scheme for classifying motifs of biochemical oscillators (FIG. 5).

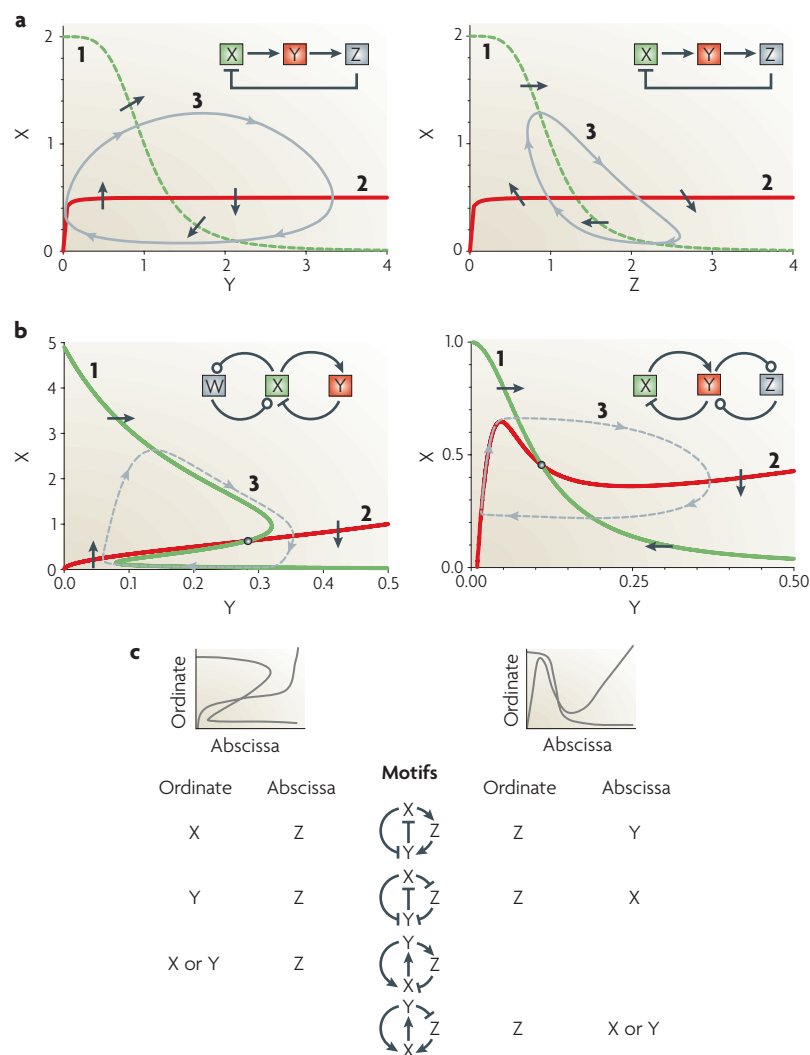


Figure 5 | A classification scheme for biochemical oscillators. We classify oscillators by their interaction motifs, where $X \rightarrow Y$ means ‘protein X activates protein Y’, $Y \rightarrow X$ means ‘Y inhibits X’, and $W \circ X$ means ‘protein W may either activate or inhibit X’. If two white circles appear in the same regulatory motif, they must have the same sign (either ++ or --). We assume that all interactions are positive or negative (not mixed mode) and that all self-interactions are negative. **a** | Class 1: delayed negative-feedback loops. Below each feedback loop, we present a state-space diagram in the style of FIG. 1d. We plot ‘activator’ X versus ‘inhibitor’ Y (left) or Z (right). Curve 3 is a projection of the limit cycle oscillation onto the XY plane. **b** | Class 2: amplified negative-feedback loops. Either the activator X can be amplified by positive feedback with W (left), or the inhibitor Y can be amplified by positive feedback with Z (right). For each motif, we plot the limit cycle oscillation (curve 3) on the XY plane. **c** | Class 3: incoherently amplified negative-feedback loops. Each motif consists of a three-component negative-feedback loop (oscillatory) and a two-component positive-feedback loop (amplifying). Each motif also contains an incoherent feed-forward loop that can originate from either X or Y. To the left and right of each motif we indicate how the state-space diagram will appear, depending on which variable is plotted on the abscissa and which is plotted on the ordinate.

First, we conjecture that oscillators always involve a negative-feedback loop. We know of no examples of chemical oscillations without negative feedback, and negative feedback seems necessary to close a sequence of chemical states back on itself. In all our examples, we will use the letter X to denote the ‘activator’ and Y to denote the ‘inhibitor’ in the negative-feedback loop;

that is, X ‘activates’ Y and Y ‘inhibits’ X. The activation or inhibition can be indirect; that is, through an intermediate, Z.

Second, we limit our study to mechanisms that lack autocatalysis (that is, cases in which component X directly promotes its own activity). We can think of a few examples (a protein kinase that phosphorylates and activates itself, or a misfolded protein that induces other copies of itself to misfold), but direct autocatalysis of this sort is rare compared to self-promotion by a positive-feedback loop (for example, X activates W and W activates X). Direct autocatalysis can be incorporated into the scheme we are presenting, but it makes the enumeration of cases unnecessarily complex.

We have already shown that the capacity to oscillate (in networks that lack direct autocatalysis) requires at least three chemical species to interact by at least three regulatory links (activation or inhibition). Motifs A and B above show two simple examples: a three-component negative-feedback loop and a pair of coupled positive- and negative-feedback loops (three components and four links). We have systematically surveyed all three-component regulatory motifs with three or four interaction links and have investigated each topologically distinct motif for the capacity to oscillate. The oscillatory motifs we found can be divided into three classes.

Class 1: delayed negative-feedback loops. By delayed negative feedback, we refer to three or more components connected in a single loop by positive and negative links, with an odd number of inhibitory links. Delayed negative feedback is often used to model oscillatory responses in molecular cell biology. Besides circadian oscillations of PER protein in fruit flies (mentioned earlier), other examples include oscillations of p53 in response to ionizing radiation^{37–40} ($p53 \rightarrow MDM2 \text{ mRNA} \rightarrow MDM2 \text{ protein} \rightarrow p53$) and oscillations of nuclear factor- κB (NF- κB) in response to stimulation by tumour necrosis factor^{40–43} ($NF-\kappa B \rightarrow IkB \text{ (inhibitor of NF-}\kappa B) \text{ mRNA} \rightarrow IkB \text{ protein} \rightarrow NF-\kappa B$).

Because this regulatory motif has three or more components, it cannot be adequately represented by a two-variable state space, as in FIGS 2b,3b. Nonetheless, it is instructive to plot trajectories of the basic motif ($X \rightarrow Y \rightarrow Z \rightarrow X$) in the XY plane (FIG. 5a, left) and in the XZ plane (FIG. 5a, right), and to compare these plots with a two-component negative-feedback loop ($X \rightarrow Y \rightarrow X$) in FIG. 2b. In FIG. 2b, curves 1 and 2 (called ‘nullclines’) indicate places where the flow of the reaction system is horizontal (in the Y direction only) and where it is vertical (in the X direction only). (Please notice that we always plot the activator X on the vertical axis.) These ‘flow indicators’ force the trajectories (the dashed curves in FIG. 2b) to spiral into the steady state. For the case of a delayed feedback loop, the trajectories do not obey the flow indicators (FIG. 5a). When we plot X versus Y (FIG. 5a, left panel), the limit cycle trajectory (curve 3) does not cross curve 1 in a horizontal direction because the rate of synthesis of X depends on the concentration of Y some time in the past (because Y’s inhibitory effect on X passes through the intermediary

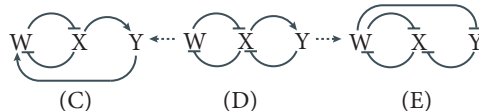
component Z). If we are plotting X versus Z (FIG. 5a, right panel), the limit cycle trajectory does not cross curve 2 in a vertical direction because the rate of synthesis of Z depends on the concentration of X some time in the past (because X's activation of Z must pass through the intermediary component Y). In both cases, the delay allows the trajectory to form a closed orbit around the steady state instead of spiralling into it.

Class 2: amplified negative-feedback loops. In FIG. 3 we considered a special case whereby the inhibitor (the protein) is amplified by a positive-feedback loop. It should be obvious that activator amplification can be just as effective. For the case of activator amplification (FIG. 5b, left panel), the X-nullcline (curve 1) is 'kinked' by the positive-feedback loop. For inhibitor amplification (FIG. 5b, right panel), the Y-nullcline (curve 2) is 'kinked'. In either case, trajectories are now forced to wheel around the steady state onto a closed orbit (curve 3, a sustained oscillation).

Where do the 'kinks' come from? A two-component positive-feedback loop ($W \rightarrow X \rightarrow W$ or $W \rightarrow X \rightarrow Y$) can respond in a bistable manner to inhibition by Y. (In this case (FIG. 5b, left) we think of Y as signal strength and X as the response variable.) If Y is large then X will be small, and if Y is small then X might be large. But for intermediate values of Y, the steady-state concentration of X can be either large or small, depending on how the system got to the intermediate value of Y. This bistability is reflected in the Z-shaped nullcline (curve 1) on the left of FIG. 5b. For the case of inhibitor amplification (FIG. 5b, right), we think of X as signal strength and Y as the response variable. In this case, Y can be a multivalued function of X, and the Y-nullcline (curve 2) becomes N-shaped. In either case, the negative feedback between X and Y forces trajectories to rotate clockwise on our standard XY plane, and the positive-feedback loop puts kinks in one of the nullclines to prevent trajectories from spiralling into the steady state.

This class of oscillators appears commonly in the literature, from the earliest models of chemical oscillations^{44–46} to recent models of mitosis-promoting factor (MPF) in frog egg extracts^{47,48}. The latter case is an activator-amplified negative-feedback loop, in which W is Cdc25, X is MPF and Y is Cdc20. An inhibitor-amplified negative-feedback loop (in which X is Cdc10, Y is Cig2 and Z is Rum1) has been used by Novak and Tyson⁴⁹ to model endoreplication (periodic DNA synthesis in the absence of cell division) in mutant fission yeast cells. Recently, a synthetic oscillator based on an activator-amplified negative-feedback loop was built in bacteria by Jeff Hasty's group⁵⁰.

Class 3: incoherently amplified negative-feedback loops. By rewiring an activator-amplified negative-feedback loop (D), we create new regulatory motifs (C and E) that may also have the potential to oscillate:



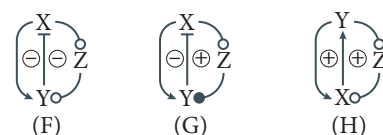
Motifs C and E both have a two-component positive-feedback loop (—, in both C and E) that is embedded in a three-component negative-feedback loop (++– in C and –– in E). Motif C also has the characteristic that X inhibits W directly and activates W indirectly (through Y). This characteristic is called an incoherent feedforward loop (C'). Motif E can also be redrawn as an incoherent feedforward loop (E').



Hence, we describe these motifs as incoherently amplified negative-feedback loops. In both motifs C' and E', the embedded positive-feedback loop is '—'. There are two other incoherently amplified negative-feedback loops based on an embedded (++) feedback loop. The four cases are shown in FIG. 5c. In each case, the negative-feedback loop can oscillate in its own right, but the additional positive-feedback loop adds bistability and robustness to the mechanism⁵¹.

The earliest models of glycolytic oscillations^{52–54} belong to this class of oscillators (FIG. 5c, fourth motif). In this motif, $Z \rightarrow X$ refers to the biochemical reaction that converts fructose-6-phosphate + ATP (Z) into fructose-1,6-bisphosphate + ADP (X). The enzyme that catalyses this reaction, phospho-fructokinase (species Y in the motif), is activated by ADP ($X \rightarrow Y$), and the active form of Y promotes both the removal of Z ($Y \rightarrow Z$) and the production of X ($Y \rightarrow X$). The Martiel–Goldbeter⁵⁵ model of cAMP oscillations in slime mould cells is another example of the fourth motif in FIG. 5c. In this case, intracellular cAMP is the activator (X) and extracellular cAMP is the incoherent signaller (Y). Extracellular cAMP binds to a membrane receptor that quickly activates the enzyme that synthesizes cAMP from ATP inside the cell. This is the fast activating signal from Y to X. Furthermore, extracellular cAMP pushes the membrane receptor (Z) into an inactive state, which only slowly recovers activity after cAMP is destroyed by extracellular phosphodiesterase. This is the slow inhibitory signal from Y to X. Tyson and Novak^{56,57} use incoherently amplified (—) negative-feedback loops (the first and second motif in FIG. 5c) to model cell-cycle transitions (M–G1 and G1–S, respectively). To model oscillations in p53 (a transcription factor that coordinates intracellular responses to DNA damage), Ciliberto *et al.*⁵⁸ used an incoherently amplified (—) negative-feedback loop and Zhang *et al.*⁵⁹ suggested an alternative mechanism based on an incoherently amplified (++) negative-feedback loop.

Other possibilities? There are three other regulatory motifs with three components, four links and a topology similar to motifs C' and E':



In these motifs, we use circles to indicate interactions of either sign (+ or -); two white circles must have the same sign, whereas black and white circles have opposite signs.

Motif F is a 'coherently repressed' negative-feedback loop that consists of two negative-feedback loops, one with three components and the other with two components. If the link $X \rightarrow Y$ is weak enough, the three-component negative-feedback loop might oscillate on its own. Addition of the two-component negative-feedback loop dampens the propensity of the three-component negative-feedback loop to oscillate.

Motif G is a different sort of incoherently amplified negative-feedback loop; it differs from the class 3 motifs in FIG. 5c in that the positive loop has three components (rather than two) and the negative loop has two components (rather than three). Everything we have said so far might lead us to expect oscillations in this motif under the right choice of nonlinearities and rate constants. However, it is possible to show that motif G cannot generate oscillations for any choice of nonlinear rate equations or any parameter settings ([Supplementary information S3](#) (box)).

Motif H has two positive-feedback loops, one with two components and one with three. We might expect this regulatory motif to exhibit bistability but not oscillations, and indeed this is the case ([Supplementary information S4](#) (box)).

More complex topologies and oscillatory behaviours. We have exhausted all possible oscillatory motifs with three components and at most four links. Topologies with three components and five or six links are so densely connected that it is difficult to think of them as regulatory 'motifs'. For example, motif I combines a class 2 inhibitor-amplified negative-feedback loop with a class 1 three-component negative-feedback loop. Either submotif can oscillate by its own right. Motif I has recently been used by Rust *et al.*⁶⁰ to model circadian oscillations in the phosphorylation state of the KaiC protein in cyanobacteria. In this case, X is KaiC phosphorylated only on the Thr residue or on both the Thr and the Ser residues, Y is KaiC phosphorylated only on the Ser residue and Z is KaiA.



Allowing for four components and five or six links opens new possibilities that we have not explored systematically. Some oscillatory motifs are simple generalizations of topologies that we have seen before. For example, motif J is an activator-amplified negative-feedback loop (class 2); the only difference from the motifs in FIG. 5b is that the negative-feedback loop has been extended to three components. This motif can oscillate⁶¹.

By combining two or more oscillatory motifs in a common mechanism it is possible to create exotic behaviour, including chaos, as illustrated in FIG. 6. FIG. 6a, adapted from Rössler's classic paper⁶² on chemical chaos, presents two overlapping 'activator amplification' oscillators ($W \rightarrow X_{-Y_1}$ and $W \rightarrow X_{-Y_2}$) that share a common activator.

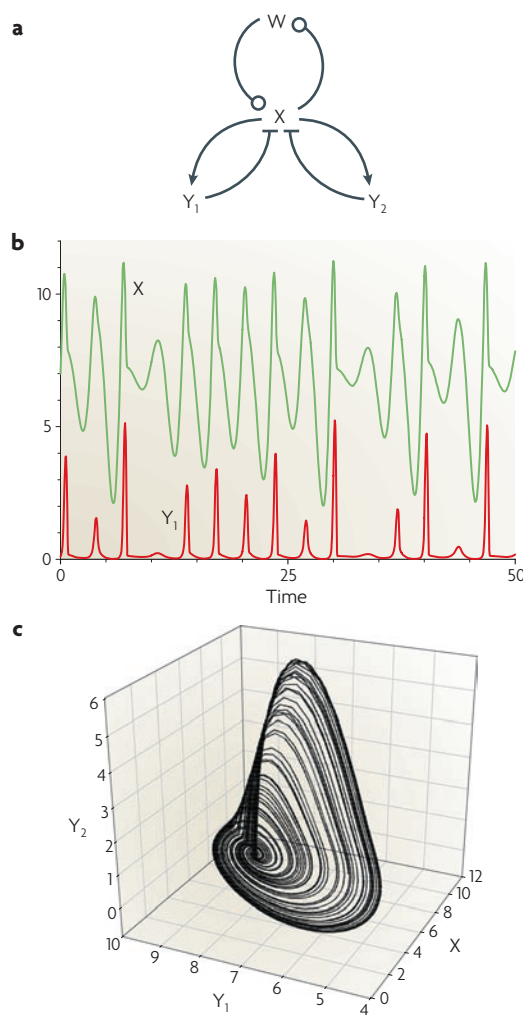


Figure 6 | Chaotic oscillators. **a** | Activator amplification with two negative-feedback loops in parallel. $W \rightarrow X$ means 'protein W may either activate or inhibit protein X'. **b** | Chaotic trajectory for the mechanism in panel **a**. [Supplementary information S1](#) (box) for details. **c** | Projection of the chaotic trajectory into the three-dimensional state space (X, Y_1, Y_2). The chaotic trajectory was recomputed from the equations and parameter values in REF. 62.

As FIG. 6b shows, the time course of X fluctuates up and down but never repeats itself. Viewing a trajectory in ($X-Y_1-Y_2$) space (FIG. 6c), we see that the curve never closes on itself (it is not periodic) and seems to sweep out a surface of complex topology.

It is beyond the scope of this review to go further into the subtleties of deterministic chaos, except to point out that the requirements for chaos seem to be undemanding. Chaotic trajectories readily arise in systems of coupled oscillators. Since multiple, coupled oscillators are likely to be common companions in the complex reaction networks underlying cell physiology, it is surprising that deterministic chaos has not been identified more often in experimental data⁵. Perhaps the chaotic trajectories of individual cells are averaged out when large populations of cells are monitored. When the behaviour of single cells

Chemical chaos

Refers to oscillatory chemical systems with aperiodic unpredictable behaviour. Chaos requires at least three interacting components.

is monitored with fluorescent proteins, the possibility of deterministic chaos is likely to be swamped by the white noise of molecular fluctuations in small volumes (a single cell). Nonetheless, experimentalists and theoreticians should be open to the possibility of deterministic chaos in their data and in their models of complex reaction networks with multiple sources of oscillation.

Summing up

By modelling specific examples of oscillatory processes, we have drawn a number of general conclusions about the design principles of biochemical oscillators. All biochemical oscillators are built around some sort of negative-feedback loop ($X \rightarrow Y \rightarrow \dots \rightarrow X$), which ensures that if the concentration of X gets too large it will eventually decrease, and if it gets too small it will eventually increase⁶³. Negative feedback is often used in biochemistry to achieve homeostasis (a stable steady state of intermediate X), but under certain conditions the steady state can lose stability and be replaced by spontaneous oscillations of X (high \rightarrow low \rightarrow high \rightarrow low \rightarrow ...). The conditions for oscillation are: sufficient nonlinearity in the reaction kinetics, sufficient 'memory' in the negative-feedback loop, and proper balancing of the timescales of components in the loop. In biochemical reaction kinetics there are many sources of nonlinearity that are conducive to oscillations (FIG. 4). 'Memory' might be a simple consequence of a long negative-feedback loop, but more likely it stems from positive-feedback loops in the biochemical reaction mechanism. When positive feedback creates two alternative stable steady states in the reaction dynamics, the system can 'remember' its recent history and thereby overshoot and undershoot the homeostatic tendencies of the negative-feedback loop.

With these ideas in mind we classify biochemical oscillators according to the topology of the positive- and negative-feedback loops in the reaction mechanism. For systems with three components and three or four links (but no self-activation links), we identify three classes of oscillators: delayed negative-feedback loops, amplified negative-feedback loops and incoherently amplified negative-feedback loops. Our classification scheme is by no means complete, and oscillator motifs may be more complicated than any of our classes. Also, we have

neglected mixed-mode effects (for example, Y activates the synthesis of X at low concentration and inactivates it at high concentration). Mixed-mode interactions might easily generate complex oscillations and chaos²¹.

If a reaction mechanism contains one of the regulatory motifs we have identified, then it can exhibit oscillatory behaviour, provided the rate constants are properly tuned. Because interaction motifs and reaction rate constants are under genetic control, it is possible for biochemical oscillators to evolve. Indeed, it is likely that biochemical oscillations have arisen repeatedly from basic, homeostatic, negative-feedback loops by serendipitous genetic changes that destabilized the steady state and generated sustained oscillations. Maladaptive oscillations would have been quickly weeded out by selection, but weakly deleterious or adventitious oscillations might have been co-opted by evolving populations for beneficial physiological purposes. Almost surely, mechanisms of circadian rhythms evolved many times independently in this way. On the other hand, bistability and oscillations that govern cell-cycle events are much more highly constrained, and the underlying mechanism (which seems to be universal across all eukaryotic cells) must have been derived from a single common ancestor.

Another consequence of the fact that a given interaction motif may or may not oscillate, depending on subtle balancing of reaction rates, is the possibility of a class of 'dynamical diseases' as distinct from 'genetic diseases'. In a genetic disease, such as sickle cell anaemia, a mutant gene encodes a defective protein that cannot do its essential job in some important aspect of physiology. In a dynamical disease, a mutant gene encodes a modified protein that still does its job but at a different rate, thereby causing a homeostatic control mechanism to break out into pathological oscillations or causing an oscillatory control system to spiral into a stable steady state⁶⁹. Some cyclic blood disorders might be dynamical diseases of the first kind, and some sleep disorders might be dynamical diseases of the second kind.

We hope that this review will help biochemists and molecular biologists to understand better the mechanisms that underlie cellular oscillations and to recognize the importance of quantitative modelling in studying these oscillations.

1. Pye, K. & Chance, B. Sustained sinusoidal oscillations of reduced pyridine nucleotide in a cell-free extract of *Saccharomyces carlsbergensis*. *Proc. Natl Acad. Sci. USA* **55**, 888–894 (1966).
2. Hess, B. & Boiteux, A. Oscillatory phenomena in biochemistry. *Annu. Rev. Biochem.* **40**, 237–258 (1971).
3. Gerisch, G., Fromm, H., Huesgen, A. & Wick, U. Control of cell-contact sites by cyclic AMP pulses in differentiating *Dictyostelium* cells. *Nature* **255**, 547–549 (1975).
4. Olsen, L. F. & Degn, H. Oscillatory kinetics of the peroxidase-oxidase reaction in an open system. Experimental and theoretical studies. *Biochim. Biophys. Acta* **523**, 321–334 (1978).
5. Olsen, L. F. & Degn, H. Chaos in an enzyme reaction. *Nature* **267**, 177–178 (1977).
6. Higgins, J. Theory of oscillating reactions. *Ind. Eng. Chem.* **59**, 19–62 (1967).
An early but still useful review on biochemical oscillators with clear explanations of the underlying theory.
7. Prigogine, I., Lefever, R., Goldbeter, A. & Herschkowitz-Kaufman, M. Symmetry breaking instabilities in biological systems. *Nature* **223**, 913–916 (1969).
8. Dunlap, J. C. Molecular bases for circadian clocks. *Cell* **96**, 271–290 (1999).
9. Evans, T., Rosenthal, E. T., Youngblom, J., Distel, D. & Hunt, T. Cyclin: a protein specified by maternal mRNA in sea urchin eggs that is destroyed at each cleavage division. *Cell* **33**, 389–396 (1983).
10. Gerhart, J., Wu, M. & Kirschner, M. Cell cycle dynamics of an M-phase-specific cytoplasmic factor in *Xenopus laevis* oocytes and eggs. *J. Cell Biol.* **98**, 1247–1255 (1984).
11. Elowitz, M. B. & Leibler, S. A synthetic oscillatory network of transcriptional regulators. *Nature* **403**, 335–338 (2000).
The first example of a synthetic GRN with oscillatory dynamics. The oscillation arises from a three-component negative-feedback loop.
12. Chance, B., Pye, E. K., Ghosh, A. K. & Hess, B. *Biological and Biochemical Oscillations* (Academic Press, New York, 1973).
13. Gray, P. & Scott, S. K. *Chemical Oscillations and Instabilities* (Clarendon Press, Oxford, 1994).
14. Goldbeter, A. *Biochemical Oscillations and Cellular Rhythms* (Cambridge University Press, Cambridge, 1996).
15. Epstein, I. R. & Pojman, J. A. *An Introduction to Nonlinear Chemical Dynamics* (Oxford University Press, Oxford, 1998).
16. Berridge, M. J. & Rapp, P. E. A comparative survey of the function, mechanism and control of cellular oscillators. *J. Exp. Biol.* **81**, 217–279 (1979).
17. Goldbeter, A. Computational approaches to cellular rhythms. *Nature* **420**, 238–245 (2002).
18. Kholodenko, B. N. Cell-signalling dynamics in time and space. *Nature Rev. Mol. Cell Biol.* **7**, 165–176 (2006).
19. Hardin, P. E., Hall, J. C. & Rosbash, M. Feedback of the *Drosophila* period gene product on circadian cycling of its messenger RNA levels. *Nature* **343**, 536–540 (1990).
One of the first demonstrations that a transcriptional negative-feedback loop is at the heart of the circadian clock.

20. Gallego, M. & Virshup, D. M. Post-translational modifications regulate the ticking of the circadian clock. *Nature Rev. Mol. Cell Biol.* **8**, 139–148 (2007).
21. Mackey, M. C. & Glass, L. Oscillation and chaos in physiological control systems. *Science* **197**, 287–289 (1977).
A classic study of oscillations in a time-delayed negative-feedback loop with application to physiological control systems.
22. Griffith, J. S. Mathematics of cellular control processes. I. Negative feedback to one gene. *J. Theor. Biol.* **20**, 202–208 (1968).
23. Goodwin, B. C. Oscillatory behavior in enzymatic control processes. *Adv. Enzyme Regul.* **3**, 425–438 (1965).
The first theoretical investigation of oscillations in a transcriptional negative-feedback loop.
24. Goodwin, B. C. An entrainment model for timed enzyme syntheses in bacteria. *Nature* **209**, 479–481 (1966).
25. Masters, M. & Donachie, W. D. Repression and the control of cyclic enzyme synthesis in *Bacillus subtilis*. *Nature* **209**, 476–479 (1966).
26. Goldbeter, A. A model for circadian oscillations in the *Drosophila* period protein (PER). *Proc. Biol. Sci.* **261**, 319–324 (1995).
27. Leloup, J. C. & Goldbeter, A. Modeling the circadian clock: from molecular mechanism to physiological disorders. *Bioessays* **30**, 590–600 (2008).
28. Thomas, R. & D’Ari, R. *Biological Feedback* (CRC Press, Boca Raton, 1990).
29. Laurent, M. & Kellershohn, N. Multistability: a major means of differentiation and evolution in biological systems. *Trends Biochem. Sci.* **24**, 418–422 (1999).
30. Tyson, J. J., Hong, C. I., Thron, C. D. & Novak, B. A simple model of circadian rhythms based on dimerization and proteolysis of PER and TIM. *Biophys. J.* **77**, 2411–2417 (1999).
31. Segel, L. A. *Biological Kinetics* (Cambridge University Press, Cambridge, 1991).
32. Monod, J., Wyman, J. & Changeux, J. P. On the nature of allosteric transitions: a plausible model. *J. Mol. Biol.* **12**, 88–118 (1965).
33. Goldbeter, A. & Koshland, D. E., Jr. An amplified sensitivity arising from covalent modification in biological systems. *Proc. Natl Acad. Sci. USA* **78**, 6840–6844 (1981).
34. Gunawardena, J. Multisite protein phosphorylation makes a good threshold but can be a poor switch. *Proc. Natl Acad. Sci. USA* **102**, 14617–14622 (2005).
35. Thron, C. D. Mathematical analysis of binary activation of a cell cycle kinase which down-regulates its own inhibitor. *Biophys. Chem.* **79**, 95–106 (1999).
36. Kim, S. Y. & Ferrell, J. E., Jr. Substrate competition as a source of ultrasensitivity in the inactivation of Wee1. *Cell* **128**, 1133–1145 (2007).
37. Lahav, G. *et al.* Dynamics of the p53–Mdm2 feedback loop in individual cells. *Nature Genet.* **36**, 147–150 (2004).
38. Lev Bar-Or, R. *et al.* Generation of oscillations by the p53–Mdm2 feedback loop: a theoretical and experimental study. *Proc. Natl Acad. Sci. USA* **97**, 11250–11255 (2000).
39. Ma, L. *et al.* A plausible model for the digital response of p53 to DNA damage. *Proc. Natl Acad. Sci. USA* **102**, 14266–14271 (2005).
40. Monk, N. A. Oscillatory expression of Hes1, p53, and NF- κ B driven by transcriptional time delays. *Curr. Biol.* **13**, 1409–1413 (2003).
41. Nelson, D. E. *et al.* Oscillations in NF- κ B signaling control the dynamics of gene expression. *Science* **306**, 704–708 (2004).
42. Cheong, R., Hoffmann, A. & Levchenko, A. Understanding NF- κ B signaling via mathematical modeling. *Mol. Syst. Biol.* **4**, 192 (2008).
43. Hoffmann, A., Levchenko, A., Scott, M. L. & Baltimore, D. The I κ B–NF- κ B signaling module: temporal control and selective gene activation. *Science* **298**, 1241–1245 (2002).
44. Franck, U. F. Kinetic feedback processes in physico-chemical oscillatory systems. *Faraday Symp. Chem. Soc.* **9**, 137–149 (1974).
45. Rössler, O. E. A principle for chemical multivibration. *J. Theor. Biol.* **36**, 413–417 (1972).
46. Gierer, A. & Meinhardt, H. A theory of biological pattern formation. *Kybernetik* **12**, 30–39 (1972).
47. Novak, B. & Tyson, J. J. Numerical analysis of a comprehensive model of M-phase control in *Xenopus oocyte* extracts and intact embryos. *J. Cell Sci.* **106**, 1153–1168 (1993).
48. Pomeroy, J. R., Kim, S. Y. & Ferrell, J. E., Jr. Systems-level dissection of the cell-cycle oscillator: bypassing positive feedback produces damped oscillations. *Cell* **122**, 565–578 (2005).
Convincing experimental evidence that amplification (positive feedback) makes the cell-cycle oscillator (a negative-feedback loop) more robust.
49. Novak, B. & Tyson, J. J. Modeling the control of DNA replication in fission yeast. *Proc. Natl Acad. Sci. USA* **94**, 9147–9152 (1997).
50. Stricker, J. *et al.* A fast, robust, and tunable synthetic gene oscillator. *Nature* (in the press).
51. Tsai, T. Y. *et al.* Robust, tunable biological oscillations from interlinked positive and negative feedback loops. *Science* **321**, 126–129 (2008).
52. Goldbeter, A. & Lefever, R. Dissipative structures for an allosteric model. Application to glycolytic oscillations. *Biophys. J.* **12**, 1302–1315 (1972).
53. Higgins, J. A chemical mechanism for oscillation of glycolytic intermediates in yeast cells. *Proc. Natl Acad. Sci. USA* **51**, 989–994 (1964).
54. Sel’kov, E. E. Self-oscillation in glycolysis. 1. A simple kinetic model. *Eur. J. Biochem.* **4**, 79–86 (1968).
55. Martiel, J. L. & Goldbeter, A. A model based on receptor desensitization for cyclic AMP signaling in *Dictyostelium* cells. *Biophys. J.* **52**, 807–828 (1987).
56. Tyson, J. J. & Novak, B. Regulation of the eukaryotic cell cycle: molecular antagonism, hysteresis, and irreversible transitions. *J. Theor. Biol.* **210**, 249–263 (2001).
57. Tyson, J. J. & Novak, B. Temporal organization of the cell cycle. *Curr. Biol.* **18**, R759–R768 (2008).
58. Ciliberto, A., Novak, B. & Tyson, J. J. Steady states and oscillations in the p53/Mdm2 network. *Cell Cycle* **4**, 488–493 (2005).
59. Zhang, T., Brazhnik, P. & Tyson, J. J. Exploring mechanisms of the DNA-damage response: p53 pulses and their possible relevance to apoptosis. *Cell Cycle* **6**, 85–94 (2007).
60. Rust, M. J., Markson, J. S., Lane, W. S., Fisher, D. S. & O’Shea, E. K. Ordered phosphorylation governs oscillation of a three-protein circadian clock. *Science* **318**, 809–812 (2007).
61. Borisuk, M. T. & Tyson, J. J. Bifurcation analysis of a model of mitotic control in frog eggs. *J. Theor. Biol.* **195**, 69–85 (1998).
62. Rössler, O. E. Chaos in abstract kinetics: two prototypes. *Bull. Math. Biol.* **39**, 275–289 (1977).
63. Snoussi, E. H. Necessary conditions for multistationarity and stable periodicity. *J. Biol. Sys.* **6**, 3–9 (1998).
64. Goldbeter, A. Mechanism for oscillatory synthesis of cyclic AMP in *Dictyostelium discoideum*. *Nature* **253**, 540–542 (1975).
65. Meyer, T. & Stryer, L. Molecular model for receptor-stimulated calcium spiking. *Proc. Natl Acad. Sci. USA* **85**, 5051–5055 (1988).
66. Garmendia-Torres, C., Goldbeter, A. & Jacquet, M. Nucleocytoplasmic oscillations of the yeast transcription factor Msn2: evidence for periodic PKA activation. *Curr. Biol.* **17**, 1044–1049 (2007).
67. Jacquet, M., Renault, G., Lallet, S., De Mey, J. & Goldbeter, A. Oscillatory nucleocytoplasmic shuttling of the general stress response transcriptional activators Msn2 and Msn4 in *Saccharomyces cerevisiae*. *J. Cell Biol.* **161**, 497–505 (2003).
68. Lewis, J. Autoinhibition with transcriptional delay: a simple mechanism for the zebrafish somitogenesis oscillator. *Curr. Biol.* **13**, 1398–1408 (2003).
69. Glass, L. & Mackey, M. C. Pathological conditions resulting from instabilities in physiological control systems. *Ann. N.Y. Acad. Sci.* **316**, 214–235 (1979).

Acknowledgements

J.J.T. acknowledges financial support from the National Institutes of Health and the hospitality of Merton College, Oxford, UK, during the writing of this review. B.N. acknowledges support from the Biotechnology and Biological Sciences Research Council and from the European Commission Seventh Framework Programme (EC FP7). Our understanding of biochemical oscillations has developed over many years of delightful conversations with A. Goldbeter, L. Segel, A. Winfree, M. Mackey and L. Glass.

DATABASES

UniProtKB: <http://ca.expasy.org/sprot>
Cdc10 | Cdc20 | Cig2 | I κ B | MDM2 | NF- κ B | p53 | PER | Rum1

FURTHER INFORMATION

Béla Novák’s homepage: <http://www.bioch.ox.ac.uk/aspsite/research/brochure/Novak>
John Tyson’s homepage: <http://mpf.biol.vt.edu/Tyson%20Lab.html>

SUPPLEMENTARY INFORMATION

See online article: S1 (box) | S2 (box) | S3 (box) | S4 (box)

ALL LINKS ARE ACTIVE IN THE ONLINE PDF

Supplementary information S1 (box): Computer programmes

Purpose: to provide 'ode' files for simulating all models in the text, using WinPP or XPP-Aut. These programs are freely available at:

<http://www.math.pitt.edu/~bard/bardware/>
<http://www.math.pitt.edu/~bard/xpp/xpp.html>

Figure 1c,d

```
# protein inhibits its own synthesis with explicit time delay
# protein is degraded by a protease according to Michaelis-Menten kinetics

dy/dt = k1*S*Kd^p/(Kd^p + delay(y,tau)^p) - k2*ET*y/(Km + y)

aux dly = delay(y,tau)
aux Fy=k1*S*Kd^p/(Kd^p + delay(y,tau)^p)

p k1=1, S=1, Kd=1, p=2, tau=10
p k2=1, ET=1, Km=1

@ XP=t, YP=y, TOTAL=100, METH=stiff, XLO=0, XHI=100, YLO=0, YHI=3.5,
delay=20
done
```

Figure 2b

```
# model for a simple negative feedback loop
# protein (y) inhibits the synthesis of its mRNA (x)

dx/dt = k1*S*Kd^p/(Kd^p + y^p) - kdx*x
dy/dt = ksy*x - k2*ET*y/(Km + y)

p k1=0.1, S=1, Kd=1, kdx=0.1, p=2
p ksy=1, k2=1, ET=1, Km=1

@ XP=y, YP=x, TOTAL=100, METH=stiff, XLO=0, XHI=4, YLO=0, YHI=1.05
done
```


Figure 2d–f

```
# Negative feedback loop with nuclear transport
# mRNA is synthesized in the nucleus (xn) and transported into the cytoplasm (xc)
# where it gets translated into protein (yc) which is translocated into the nucleus (yn)
#
# eps = Vnuc/Vcyt
# half-life of mRNA in nucleus = 0.693/kdxn
# half-life of prot in cytoplasm = 0.693/kdyc

dxn/dt = kdxn*(sig/(1 + yn^p) - xn) - kexport*xn
dxc/dt = eps*kexport*xn - kdxk*xc
dyc/dt = kdyc*(xc - yc) - eps*kimport*yc
dyn/dt = kimport*yc - kdyn*yn/(Km + yn)

p Sig=1000, p=2, kdxn=10, kexport=0.2,kdxk=0.2, eps=1
p kdyn=8, kdyc=0.1, Km=0.1, kimport=0.1

@ XP=t, YP=xn, TOTAL=100, METH=stiff, XLO=0, XHI=100, YLO=0,
YHI=1000, bounds=10000
done
```

Figure 3b–f

```
# protein inhibits its own degradation

dx/dt = k1*S*Kd^p/(Kd^p + y^p) - kdx*x
dy/dt = ksy*x - kdy*y - k2*ET*y/(Km + y + KI*y^2)

p S=1, k1=0.05, Kd=1, p=4, kdx=0.05
p ksy=1, kdy=0.05, k2=1, ET=1, Km=0.1, KI=2

@ XP=y, YP=x, TOTAL=250, METH=stiff, XLO=0, XHI=4, YLO=0, YHI=1.05
done
```

Figure 5a (left)

Three component negative feedback oscillator (+ + -)

X -> Y -> Z -| X

$$dx/dt = k_{sx} * S / (1 + z^p) - k_{dx} * x$$

$$dy/dt = k_1 * x - k_2 * y / (K_m + y)$$

$$dz/dt = k_3 * (y - z)$$

$$p \text{ } k_{sx}=0.1, S=2, k_{dx}=0.1, p=4$$

$$p \text{ } k_1=0.2, k_2=0.1, K_m=0.01, k_3=0.05$$

@ XP=t, YP=x, TOTAL=250, METH=stiff, XLO=0, XHI=250, YLO=0, YHI=1
done

Figure 5b (left)

Activator amplification & negative feedback

$$dx/dt = k_{sx}' + k_{sx} * w - (k_{dx}' + k_{dx} * y) * x$$

$$dy/dt = k_{sy} * x^p / (1 + x^p) - k_{dy} * y$$

$$w = x^q / (1 + x^q)$$

$$p \text{ } k_{sx}'=0.02, k_{sx}=1, k_{dx}'=0.2, k_{dx}=1, q=2$$

$$p \text{ } k_{sy}=0.01, k_{dy}=0.01, p=2$$

@ XP=y, YP=x, TOTAL=250, METH=stiff, XLO=0, XHI=0.5, YLO=0, YHI=5
done

Figure 5b (right)

Inhibitor amplification with negative feedback

x promotes y synthesis and y promotes x degradation

y degradation is enhanced by z

y binds to z to form an inactive complex C

#

$$\# \text{ } K_{diss} * C = Y_{free} * Z_{free} = (Y_{total} - C) * (Z_{total} - C)$$

$$dx/dt = k_{sx} - (k_{dx}' + k_{dx} * y^p) * x$$

$$dy/dt = k_{sy}' + k_{sy} * x - (k_{dy}' + k_{dy} * z) * Y$$

$$BB = ZT + Y + K_{diss}$$

$$CC = 2 * ZT * Y / (BB + \sqrt{BB^2 - 4 * ZT * Y})$$

$$z = ZT - CC$$

$$p \text{ } k_{sx}=0.01, k_{dx}'=0.01, k_{dx}=1, p=2$$

p ksy'=0.1, ksy=0.2, kdy'=0.1, kdy=250, Kdiss=0.01
p ZT=0.05

@ XP=y, YP=x, TOTAL=250, METH=stiff, XLO=0, XHI=0.5, YLO=0, YHI=1
done

Figure 6b,c

Rossler (1977) BMB

#

Spiral Chaos

$dx/dt = k1 + k2*x - (k3*y+k4*z)*x/(K+x)$

$dy/dt = k5*x - k6*y$

$dz/dt = k7*x - k8*z/(L+z)$

p k1=22, k2=2.2, k3=4.4, k4=4.4, k5=1.2

p k6=1, k7=14, k8=140, K=0.01, L=0.05

init x=7, y=6, z=0.1

done

Supplementary information S2 (box): Negative feedback with explicit time delay

Purpose: to derive the constraint between τ and S for oscillatory solutions to equation (2) of the main text. The constraint equation is used to plot the curves in Fig. 1e and f.

First, we write equation (2) in dimensionless form:

$$\frac{dy(\hat{t})}{d\hat{t}} = \frac{\sigma}{1 + [y(\hat{t} - \hat{\tau})]^p} - \frac{y}{\kappa + y}, \text{ where } y(\hat{t}) = \frac{Y(t)}{K_d} \text{ and } \hat{t} = \frac{k_2 E_T}{K_d} t. \quad (\text{S2.1})$$

The parameters in this equation are defined by $\sigma = \frac{k_1 S}{k_2 E_T}$, $\kappa = \frac{K_m}{K_d}$, $\hat{\tau} = \frac{k_2 E_T}{K_d} \tau$.

The steady state solution of equation (S2.1) is the unique real positive root, y_o , of

$$y^{p+1} - (\sigma - 1)y - \sigma\kappa = 0. \quad (\text{S2.2})$$

Assume $y(\hat{t}) = y_o + ce^{i\omega\hat{t}}$, where $c = \text{constant}$. Substituting this assumed solution into equation (S2.1), we find that

$$i\omega = \rho - \phi e^{-i\omega\hat{\tau}} \quad (\text{S2.3})$$

where $\rho = \frac{\kappa}{(\kappa + y_o)^2}$ and $\phi = \frac{\sigma p y_o^{p-1}}{(1 + y_o^p)^2}$. Using (S2.2) we find a convenient relation

between ϕ and ρ : $\frac{\phi}{\rho} = p \left[1 + (\sigma - 1) \frac{y_o}{\sigma\kappa} \right] \equiv R$, where R is a label for $p[\dots]$.

Equating the real and imaginary parts of equation (S2.3), we find that

$$\rho^2 + \omega^2 = \phi^2 \text{ and } \omega\hat{\tau} = \arctan(-\omega / \rho). \quad (\text{S2.4})$$

The conditions (S2.4) imply that

$$\omega = \rho \sqrt{R^2 - 1} \text{ and } \hat{\tau} = \omega^{-1} \arctan(-\sqrt{R^2 - 1}). \quad (\text{S2.5})$$

We are now prepared to compute the curves in Fig. 1e and f, by the following pseudocode:

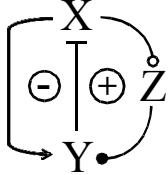
```

Scan over  $p=1, 2, 3, \dots$ 
  Scan over values of  $\kappa$ 
    Scan over values of  $\sigma$ 
      Solve (S2.2) for  $y_0$ 
      Compute  $R=p*[1+(\sigma-1)*y_0/(\sigma\kappa)]$ 
      If  $(R>1)$ , then
        Compute  $\rho=\kappa/(\kappa+y_0)^2$ 
        Compute  $\omega=\rho*\sqrt{R^2-1}$ 
        Compute  $\tau=\arctan(-\omega/\rho)/\omega$ 
        Compute  $\text{Period}=2*\pi/\omega$ 
        Save  $(\sigma, \tau, \omega, \text{Period})$ 
      Else continue
    Continue
  For each  $(p, \kappa)$ , plot  $(\tau \text{ versus } \sigma)$ 
Continue
End
  
```

Supplementary information S3 (box): Motif G

Purpose: to prove that the incoherently amplified negative feedback loop in motif (G), with a two-component negative feedback loop and a three-component positive feedback loop, cannot generate oscillations by a Hopf bifurcation.

For motif (G) proposed in the main text (also below, left), we exhibit the sign pattern of the Jacobian matrix (below, right), where the a 's, b 's and c 's are all > 0 ,

	$\mathbf{J} = \begin{pmatrix} -a_x & -a_y & 0 \\ b_x & -b_y & \mp b_z \\ \pm c_x & 0 & -c_z \end{pmatrix}$
-----------------------------------------------------------------------------------	------------------------------------------------------------------------------------------------------------

The stability of the steady state depends on the eigenvalues, λ , of the Jacobian matrix, which are the roots of the characteristic equation:

$$\begin{aligned}
 0 &= \det \begin{pmatrix} -a_x - \lambda & -a_y & 0 \\ b_x & -b_y - \lambda & \mp b_z \\ \pm c_x & 0 & -c_z - \lambda \end{pmatrix} \\
 0 &= (\lambda + a_x)(\lambda + b_y)(\lambda + c_z) + a_y b_x (\lambda + c_z) - a_y b_z c_x \\
 0 &= \lambda^3 + \lambda^2 (a_x + b_y + c_z) + \lambda (a_x b_y + b_y c_z + a_x c_z + a_y b_x) + a_x b_y c_z + a_y b_x c_z - a_y b_z c_x \\
 &\quad \text{(S3.1)}
 \end{aligned}$$

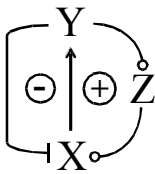
In order for a Hopf bifurcation to occur, this algebraic equation must have a pair of pure imaginary roots, $\lambda = \pm i\omega$. The necessary and sufficient condition for pure imaginary roots to equation (S3.1) is

$$\begin{aligned}
 a_x b_y c_z + a_y b_x c_z - a_y b_z c_x &= (a_x + b_y + c_z)(a_x b_y + b_y c_z + a_x c_z + a_y b_x) \\
 0 &= 2a_x b_y c_z + a_x (a_x b_y + a_x c_z + a_y b_x) + b_y (a_x b_y + b_y c_z + a_y b_x) + c_z (b_y c_z + a_x c_z) + a_y b_z c_x \\
 &\quad \text{(S3.2)}
 \end{aligned}$$

Clearly, equation (S3.2) cannot be satisfied for any choice of a_x , etc. Hence, it is impossible for this motif to generate oscillations by a Hopf bifurcation. On the other hand, $\lambda = 0$ is a possible solution of equation (S3.1), if $a_x b_y c_z + a_y b_x c_z = a_y b_z c_x$.

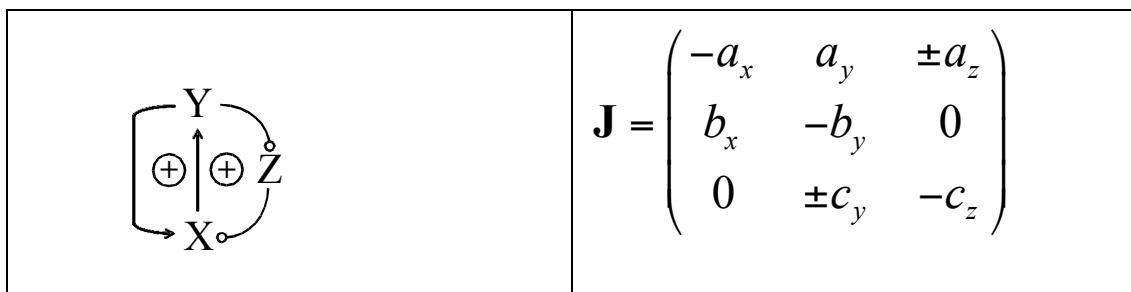
Hence, this motif can generate multiple steady states by saddle-node bifurcations. So we conclude that motif (G) can exhibit bistability but not oscillations.

By a similar argument, we can come to the same conclusion for motif (G') below

	$\mathbf{J} = \begin{pmatrix} -a_x & -a_y & \pm a_z \\ b_x & -b_y & 0 \\ 0 & \pm c_y & -c_z \end{pmatrix}$
-----------------------------------------------------------------------------------	------------------------------------------------------------------------------------------------------------

Supplementary information S4 (box): Motif H

Purpose: to prove that motif (H) (below, left), for which both the two-component and three-component feedback loops are positive, can exhibit bistability but cannot generate stable oscillations by a Hopf bifurcation.



The sign pattern of the Jacobian matrix for motif (H) is given above (right), where the a 's, b 's and c 's are all > 0 . The stability of the steady state depends on the eigenvalues, λ , of the Jacobian matrix, which are the roots of the characteristic equation:

$$\begin{aligned}
 0 &= \det \begin{pmatrix} -a_x - \lambda & a_y & \mp a_z \\ b_x & -b_y - \lambda & 0 \\ 0 & \mp c_y & -c_z - \lambda \end{pmatrix} \\
 0 &= (\lambda + a_x)(\lambda + b_y)(\lambda + c_z) - a_y b_x (\lambda + c_z) - a_z b_x c_y \\
 0 &= \lambda^3 + \lambda^2 (a_x + b_y + c_z) + \lambda (a_x b_y + b_y c_z + a_x c_z - a_y b_x) + a_x b_y c_z - a_y b_x c_z - a_z b_x c_y \\
 &\quad \text{(S4.1)}
 \end{aligned}$$

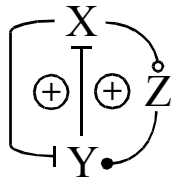
In order for a Hopf bifurcation to occur, this algebraic equation must have a pair of pure imaginary roots, $\lambda = \pm i\omega$. The necessary and sufficient condition for pure imaginary roots to equation (S4.1) is

$$\begin{aligned}
 a_x b_y c_z - a_y b_x c_z - a_z b_x c_y &= (a_x + b_y + c_z)(a_x b_y + b_y c_z + a_x c_z - a_y b_x) \\
 a_y b_x (a_x + b_y) - a_z b_x c_y &= 2a_x b_y c_z + a_x^2 (b_y + c_z) + b_y^2 (a_x + c_z) + c_z^2 (a_x + b_y) \quad \text{(S4.2)} \\
 0 &= 2a_x b_y c_z + c_z (a_x^2 + b_y^2) + c_z^2 (a_x + b_y) + a_z b_x c_y + (a_x b_y - a_y b_x)(a_x + b_y)
 \end{aligned}$$

If $(a_x b_y - a_y b_x) > 0$, then equation (S4.2) cannot be satisfied for any choice of a_x , etc. Hence, if motif (H) is to generate limit cycle oscillations by a Hopf bifurcation, then $(a_x b_y - a_y b_x)$ must be < 0 . But, in that case, the characteristic equation (S4.1) must have a real positive root, $\lambda_1 > 0$, as well as a pair of pure imaginary eigenvalues. The bifurcating limit cycles must be unstable. We conclude that it is impossible for motif (H) to generate stable oscillations by a Hopf bifurcation.

On the other hand, $\lambda = 0$ is a possible solution of equation (S4.1), if $a_x b_y c_z = a_z b_x c_y + a_y b_x c_z$. Hence, motif (H) can generate multiple steady states by saddle-node bifurcations.

By a similar argument, we can come to the same conclusion for motif (H') below:

	$\mathbf{J} = \begin{pmatrix} -a_x & -a_y & 0 \\ -b_x & -b_y & \mp b_z \\ \mp c_x & 0 & -c_z \end{pmatrix}$
-----------------------------------------------------------------------------------	-------------------------------------------------------------------------------------------------------------